R. & M. No. 2872
(14,830)
A.R.C. Technical Report

MINISTRY OF SUPPLY

AERONAUTICAL RESEARCH COUNCIL
REPORTS AND MEMORANDA

An Extension of Multhopp's Method of Calculating the Spanwise Loading of Wing-Fuselage Combinations

By

J. WEBER, Dr. rer. nat.,
D. A. KIRBY, B.Sc.,
and
D. J. KETTLE

LONDON: HER MAJESTY'S STATIONERY OFFICE
1956
SEVEN SHILLINGS NET

An Extension of Multhopp's Method of Calculating the Spanwise Loading of Wing-Fuselage Combinations

By

J. WEBER, Dr. rer. nat.,
D. A. KIRBY, B.Sc.
and
D. J. KETTLE

COMMUNICATED BY THE PRINCIPAL DIRECTOR OF SCIENTIFIC RESEARCH (AIR), MINISTRY OF SUPPLY

Reports and Memoranda No. 2872*
November, 1951

Summary.—A simple method is described for calculating the spanwise loading over wing-fuselage combinations. It is based on Multhopp's method[4], which is extended here to cover wings of finite thickness, large root chords compared with the body diameter and also swept wings. The method is restricted to wings of moderate and large aspect ratios (above about 2). The effect of different junction shapes above and below the wing in off-centre positions of the wing cannot yet be calculated. The calculation can be performed in about one computer-day, and comparisons with experimental results show good agreement in the symmetrical case.

1. *Introduction.*—The mutual interference between wing and fuselage is the oldest of the interference problems in aeronautics, yet it has not been completely solved. Recent summary reports by Schlichting[1] (1946) and by Flax and Lawrence[2] (1951) show the great variety of problems involved and the methods so far employed in dealing with them. In the past, efforts have been mainly concentrated on straight wings of fairly large aspect ratio and the aim was to predict the changes of lift and pitching moment due to the body for aerodynamic and structural purposes. In general, the main effect of the body was a reduction in lift because of the body usually being set at a negative angle relative to the no-lift line of the wing (*see, e.g.*, Becker, Squire, and Callen[3] (1943)).

The introduction of aircraft with swept wings of smaller aspect ratio (about 3) to fly at high subsonic speeds has stimulated interest in the effect of the body on the span loading. In this case, the addition of the body to the wing may often result in an increase of overall lift. Since it may be necessary to vary camber and twist along the span of a swept wing to obtain a desired span loading, the body interference effects must be known previous to this design work.

In this report, the load distribution over wing and body in incompressible non-viscous flow is treated ; the influence of viscosity is only occasionally taken into account. Compressibility effects may be treated by the Prandtl-Glauert analogy. It is considered that Multhopp's theoretical approach[4] provides a sound physical picture of the actual flow conditions, and his theory is therefore taken as a basis. However, this theory has to be extended in several respects as it is confined to thin unswept wings, the chords of which are small compared with the body diameters. In the present report it is extended to cover thick wings and larger chord-diameter

* R.A.E. Report Aero. 2446, received 25th April, 1952.

ratios. The treatment of thick wings does not allow for changes in junction shape in asymmetrical settings. Multhopp's theory is also extended to swept wings. The method is applicable to wings of moderate or large aspect ratio (above about 2). For smaller aspect ratio, an approach on the lines indicated by R. T. Jones[5] (1946) will be more appropriate.

To facilitate the use of Multhopp's theory, a brief outline of his main arguments is given first.

2. *Summary of Multhopp's Work.*—Consider an isolated body at incidence in a uniform flow. The pressure distribution over its surface produces a lift force near the nose of the body and a download near the tail; the sum of these forces is zero in non-viscous flow. To illustrate this, Fig. 1 shows the pressure distribution over the section in the plane of symmetry of an ellipsoid at incidence from exact theory and also the load distribution along its length as integrated around the circumference at sections $x = \text{const.}$ The exact theory is compared with the following approximation from the momentum theorem for slender bodies:

$$\frac{1}{\frac{1}{2}\rho V_0^2}\frac{dL(x)}{dx} = 2\pi \sin\alpha \frac{dr^2}{dx} \quad \text{for axially symmetrical bodies,} \qquad \ldots \qquad (1)$$

where $2r$ is the body diameter

$$\frac{1}{\frac{1}{2}\rho V_0^2}\frac{dL(x)}{dx} = 2 \sin\alpha \frac{dA(x)}{dx} \quad \text{for any cross-section shape,}$$

where $A(x)$ is the cross-section area. Although this approximation fails near the stagnation point the agreement is shown to be good enough for equation (1) to be used as a simple way of making an approximate estimate.

In most practical cases the centre part of the fuselage is nearly cylindrical and the fineness ratio of the fuselage is so large that the flow at the centre part is nearly the same as for an infinitely long cylindrical body, *i.e.*, no forces exist there. The flows at the nose and the tail are then separated from one another and depend mainly on the individual fineness ratios of nose and tail. This is illustrated in Fig. 2. Equation (1) gives the lift on the cylindrical middle part to be exactly zero. The lift at the body nose is still counterbalanced by the download at the tail and only a moment remains.

For a wing-body combination at incidence, the lift on the wing will be carried across the body to some extent. The flow about the body upstream and downstream of the wing will also be affected, as illustrated in Fig. 3. Upstream of the wing, the upwash induces a lift force decreasing with distance from the wing. The front part of the body is usually long enough for this lift not to overlap, or to overlap only by a small amount the lift on the nose of the body. Behind the wing, the lift induced by the wing will also fade out. The tail of the body however is always in the downwash field of the trailing vortices of the wing. Consequently, the local incidence and the download there are reduced. Apart from this effect, the lift on the body as induced by the wing can be determined by considering the body to be cylindrical and of infinite length*.

The flow about the wing is also modified by the presence of the body. With the body at an incidence α_B to the main stream, only the cross-flow component $\alpha_B V_0$ has to be considered. Because of the displacement of this flow by the body, a velocity increment is produced at the body junction and outside the body near the wing. This is in effect an additional upwash, producing a lift on the wing and existing even when the wing is at zero incidence. For long cylindrical bodies, this upwash on the wing can be determined from the two-dimensional flow

* This assumption is justified by experimental evidence, *see* sections 6 and 7.

around the body cross-section. It thus depends on the shape of the body cross-section and on the position of the wing on the body*. This is illustrated in Fig. 4 for the special case of a body with circular cross-section. As is well known, the velocity in the flow around a circle rises up to twice the free-stream velocity, *i.e.*, the maximum velocity increment is $\alpha_B V_0$ and thus the additional upwash is α_B on the body side for a mid-wing. Along the span of the wing, the additional upwash decreases as $\alpha_B/(y/R)^2$. This may be regarded as an effective twist of the wing.

The load distribution over wing and fuselage must satisfy the condition that the downwash field induced by it together with the free stream have no velocity component normal to both wing and body surfaces. This complicated three-dimensional problem is considerably simplified by assuming, in accordance with linearized theory, that the wake follows the direction of the undisturbed flow and that the load distribution can be determined by considering the spanwise section of wing plus body which is equal to the section of the wake far behind the wing in the so-called Trefftz-plane as illustrated in Fig. 5.

The circulation and thus the load distribution of this configuration can then be found if the configuration is made into a streamline in a uniform flow directed upwards in the Trefftz-plane. The load so obtained gives minimum induced drag. The solution for high aspect ratio wings was given by Lennertz[7] (1927). It is closely related to the theory of very low aspect ratio wing-body combinations by Spreiter[8] (1948), which is based on R. T. Jones' theory where the boundary conditions are also satisfied in the Trefftz-plane. The load distributions obtained by Spreiter are identical to those of Lennertz, as has been pointed out by Flax and Lawrence.

Multhopp progressed from here by making the following two suggestions:— Firstly, by using the assumption that the downwash of the trailing vortices at the wing and body is constant along the chord and equal to half its value at infinity, the boundary conditions in the Trefftz-plane can be related to those on the wing and body. The latter take account of the wing plan-form and local lift slopes C_L/α_{eff}, and thus the boundary conditions can be taken from the real wing but satisfied in the Trefftz-plane. This implies that the vortices replacing the configuration in the Trefftz-plane are still in the same position as in the minimum case, although this configuration is not a streamline. This is, of course, permissible within the linearized theory. The treatment is therefore not restricted to the minimum induced drag case only. Secondly, the configuration in the Trefftz-plane can easily be transformed into another in which the body cross-section appears as a vertical slit in the line of symmetry, which is automatically a streamline. The transformation being conformal, the potential and hence the circulation remain unaltered. This simplifies the calculation considerably compared with that of Lennertz, where the images of the vortices in the circle were considered. The boundary conditions in the Trefftz-plane and the transformation being known, the boundary conditions in the transformed Trefftz-plane are also known and the problem reduces to that of satisfying an integral equation which is of the same type as that for the load on a wing without body. The load distribution over the real wing and across the body within the wing region can then be determined by transforming back from the transformed Trefftz-plane the results obtained there by an ordinary calculation of a wing loading. For the latter Multhopp's method from Ref. 9 can conveniently be used.

3. *Outline of the Extensions of Multhopp's Method.*—Multhopp's theory can be extended to take account of wing thickness, finite ratio between wing chord and body diameter, and sweep-back.

To take the finite wing thickness properly into account a three-dimensional treatment would be necessary. To avoid this, only a rough approximation is attempted here. One effect of the finite thickness is to produce different junction shapes on the upper and lower surfaces if

* *See, e.g.*, Liess and Riegels[6] (1942), where the flow around bodies of various cross-sections has been calculated.

the wing is in an off-centre position or at an angle to the body axis. This gives an additional lift at and near the junction, which does not change with incidence. This effect is not treated in this report. With a mid-wing arrangement, the main effect of the finite thickness is to reduce the body upwash compared with that of a thin wing. Since this reduction gives a second-order term to the load distribution, only a rough approximation is needed. If body and wing are replaced by singularities (sources, doublets), only those singularities that replace the part of the body outside the wing contribute to the upwash. We take account of this fact by reducing the upwash produced by the isolated body by a factor k that is taken as constant along chord and span. k is taken equal to the ratio of the body cross-sectional area above and below the wing to the total frontal area of the body. A similar method has been used for the calculation of the interference of the body in the wing-body junction at zero lift, and satisfactory results were obtained by arbitrarily taking this factor at the maximum wing thickness ; this has again been done in the present report.

The body upwash is largest in the wing-body junction and fades out spanwise. In the case of a circular cylinder the upwash decreases from its maximum value at the junction to 1/9 of this value at a distance of one diameter from the junction. The root chord is, in general, equal to or greater than the body diameter, so that the part of the wing that is effectively twisted has an aspect ratio of one or less. The lift distribution caused by the twist produces a system of trailing vortices, for which the conditions on a small aspect ratio wing apply. We can no longer expect that the induced downwash is constant along the chord and half the value far downstream. Now the mean downwash on the chord is nearly equal to the value far downstream. The difference in the load distribution between taking half the value and taking the full value is not great enough to warrant a detailed investigation. The results of J. Ginzel[10] (1940) have been used where it has been shown that with such rapid incidence changes of small 'aspect ratio' a good approximation for the spanwise lift distribution is obtained by taking the downwash on the wing as equal to the downwash at infinity.

If in a special case the wing chord is small compared with the body diameter a second calculation can be done taking the downwash over the wing as half the value at infinity. It will be found that the two terms of the additional load distribution induced by the body upwash—which are small correction terms anyhow—differ by less than a factor 2 from one another.

Another consequence of the small 'aspect ratio' of the 'twisted' part of the wing is that the chordwise distribution of the corresponding lift increment differs from the ordinary flat-plate distribution in that the lift is concentrated near the leading edge, producing a pronounced suction peak there.

The third extension of Multhopp's theory concerns the effect of the bound vortices, which appears in the boundary conditions in the Trefftz-plane in the form of the sectional lift slope, a. For unswept flat wings the value of a is constant. This, however, is no longer true for swept wings.

Generally, the bound vortices of the wing are reflected in the body wall. In the body junction of swept wings, however, similar conditions prevail as at the centre of swept wings without body, resulting in a distortion of the chordwise loading there and in a sectional lift slope different from that of the two-dimensional aerofoil (*see* Küchemann[11] (1950)). This has been confirmed by experiments (*see* R.A.E. Wind-Tunnel Staff[12] (1949)). The value of a thus varies along the span. With the transformation of the body into the vertical slit the body junction is transformed into the centre of the wing and therefore the calculation of the lift distribution in the transformed Trefftz-plane is the same as for the ordinary swept wing. The calculation method of Küchemann[11] (1950) is used here. The effect of sweepback is thus taken into account only as a variation of the sectional lift slope along the span ; otherwise the same assumptions are made as above. The influence of the trailing vortex sheet can still be computed by using half the value of the induced downwash far behind the wing. Thus the calculation procedure for swept wings is the same as that for unswept wings.

4. *The Load Distribution over the Wing.*—4.1. *General Method of Calculation.*—The lift distribution over the wing is determined by the equation

$$C_L(y) = \left(\frac{dC_L}{d\alpha_{\text{eff}}}\right)_y . \alpha_{\text{eff}}(y)$$

$$= a(y) . \alpha_{\text{eff}}(y) \quad .. \quad .. \quad .. \quad .. \quad .. \quad (2)$$

where $a = dC_L/d\alpha_{\text{eff}}$ is the sectional lift slope. The effective incidence α_{eff} is determined by the velocity component v_z normal to the mainflow and the velocity V_0 of the main flow:—

$$\alpha_{\text{eff}} = -\frac{v_z}{V_0} . \quad .. \quad .. \quad .. \quad .. \quad .. \quad .. \quad (3)$$

The downwash can be split into three terms:

$$v_z = -\alpha_W V_0 + v_{zB} + v_{zi} \quad .. \quad .. \quad .. \quad .. \quad (4)$$

where α_W is the angle between the zero-lift line of the wing and the main flow direction, v_{zB} the upwash produced by the body and v_{zi} the velocity induced by the trailing vortices.

The velocity components v_{zB} and v_{zi} are calculated by means of a conformal transformation of the plane normal to the body axis as explained above. A rectangular co-ordinate system x,y,z is used, where the y,z-plane is normal to the axis of the fuselage and the y-axis in spanwise direction. Let

$$u = z + iy \quad .. \quad .. \quad .. \quad .. \quad .. \quad .. \quad (5)$$

be the complex variable in the Trefftz-plane and

$$\bar{u} = \bar{z} + i\bar{y} \quad .. \quad .. \quad .. \quad .. \quad .. \quad .. \quad (6)$$

the variable in the transformed Trefftz-plane, where the body cross-section is transformed into a slit parallel to the $\bar{z}$-axis. If the body is at an incidence α_B to the main flow, then the main flow in the u-plane has the velocity $-\alpha_B V_0$ parallel to the z-axis and the additional upwash produced by the isolated body is

$$v_{zB} = -\alpha_B V_0 \left[R\left(\frac{d\bar{u}}{du}\right) - 1\right]$$

$$= -\alpha_B V_0 [T(y) - 1] \quad .. \quad .. \quad .. \quad .. \quad (7)$$

where $T(y) = R(d\bar{u}/du)$ is the real part of the differential quotient $d\bar{u}/du$. We are not going to determine the conformal transformation of the body with the thick wing present. We take as an approximation for the upwash produced by a body attached to a thick wing the upwash of the isolated body reduced by a factor k, constant along the span.

$$v_{zB} = -\alpha_B V_0 k [T(y) - 1] . \quad .. \quad .. \quad .. \quad .. \quad (8)$$

In this report k is taken as the ratio of the body cross-section area above and below the wing to the total body cross-section area at the position of the maximum wing thickness; more experimental evidence may make another definition preferable.

In calculating the induced downwash v_{zi} we make use of the fact that the circulation $\Gamma(y)$ does not alter when going from the u-plane to the $\bar{u}$-plane, since it is equal to the discontinuity of the potential function Φ along the vortex sheet in the Trefftz-plane.

$$\Gamma(y) = \Gamma(\bar{y}) .$$

The induced downwash in the transformed Trefftz-plane is given by

$$\bar{v}_{zi}(x = \infty , \bar{y}) = \frac{1}{2\pi} \int_{-\bar{b}/2}^{+\bar{b}/2} \frac{d\Gamma}{d\bar{y}'} \frac{d\bar{y}'}{\bar{y} - \bar{y}'} .$$

The downwash v_{zi} in the u-plane is obtained by multiplying $\bar{v}_{zi}$ by $T(y) = R(d\bar{u}/du)$ for the thin wing:

$$v_{zi}(x = \infty , y) = \frac{1}{2\pi} T(y) \int_{-\bar{b}/2}^{+\bar{b}/2} \frac{d\Gamma}{d\bar{y}'} \frac{d\bar{y}'}{\bar{y} - \bar{y}'} . \qquad .. \quad .. \quad .. \quad (9)$$

For the thick wing we replace $T(y)$ by $T^*(y)$:

$$T^*(y) = 1 + k[T(y) - 1] \qquad .. \quad .. \quad .. \quad .. \quad (10)$$

similar to equation (8).

We introduce the non-dimensional circulation

$$\gamma(y) = \frac{\Gamma(y)}{bV_0} ; \quad \bar{\gamma}(\bar{y}) = \frac{\Gamma(\bar{y})}{\bar{b}V_0} = \frac{b}{\bar{b}} \gamma(y) \qquad .. \quad .. \quad .. \quad .. \quad (11)$$

where b and $\bar{b}$ are the wing span in the original and transformed planes, respectively. $\gamma(y)$ can be written as the sum of two terms:

(*a*) γ_W which depends on α_W and not on α_B ,

(*b*) γ_B which is proportional to α_B and independent of α_W .

Correspondingly, the downwash far downstream can be written as a sum of $v_{zi}(\gamma_W)$ and $v_{zi}(\gamma_B)$. As explained above we take the downwash induced by γ_W at the wing as $\frac{1}{2}v_{zi}(\gamma_W , x = \infty)$ and the downwash induced by γ_B at the wing as equal to $v_{zi}(\gamma_B , x = \infty)$. Together with Kutta-Joukowski's theorem:

$$\gamma(y) = \frac{\Gamma(y)}{bV_0} = \frac{C_L(y)\, c(y)}{2b} = \frac{a(y)\, c(y)}{2b} \cdot \alpha_{\text{eff}}(y) \qquad .. \quad .. \quad .. \quad (12)$$

we get from equations (3), (4), (8), (9) the final equations:

$$\bar{\gamma}_W(\bar{\eta}) = \frac{a(\bar{\eta})\, c(\bar{\eta})}{2\bar{b}} \left\{ \alpha_W(\bar{\eta}) - \frac{1}{2\pi} T^*(k,\bar{\eta}) \int_{-1}^{+1} \frac{d\bar{\gamma}_W(\bar{\eta}')}{d\bar{\eta}'} \frac{d\bar{\eta}'}{\bar{\eta} - \bar{\eta}'} \right\} \qquad .. \quad .. \quad (13)$$

$$\bar{\gamma}_B(\bar{\eta}) = \frac{a(\bar{\eta})\, c(\bar{\eta})}{2\bar{b}} \left\{ \alpha_B[T^*(k,\bar{\eta}) - 1] - \frac{1}{\pi} T^*(k,\bar{\eta}) \int_{-1}^{+1} \frac{d\bar{\gamma}_B(\bar{\eta}')}{d\bar{\eta}'} \frac{d\bar{\eta}'}{\bar{\eta} - \bar{\eta}'} \right\} \qquad .. \quad (14)$$

where the non-dimensional spanwise co-ordinate

$$\bar{\eta} = \frac{\bar{y}}{\bar{b}/2} \qquad .. \quad .. \quad .. \quad .. \quad .. \quad .. \quad (15)$$

has been introduced.

4.2. *Details of the Calculation.*—The equations (13) and (14) can be solved using the method which has been developed by Multhopp for the unswept wing, *see* Refs. 9 and 11. The integral equations are replaced by a system of linear equations:

$$\left(b_{\nu\nu} + \frac{2\bar{b}}{a(\bar{\eta}_\nu) \cdot c(\bar{\eta}_\nu)\ T^*(\bar{\eta}_\nu)}\right)\bar{\gamma}_W(\bar{\eta}_\nu) = \frac{\alpha_W(\bar{\eta}_\nu)}{T^*(\bar{\eta}_\nu)} + \sum_{n=1}^{m}{}' b_{\nu n}\bar{\gamma}_W(\bar{\eta}_n) \quad .. \quad .. \quad .. \quad (16)$$

$$\left(b_{\nu\nu} + \frac{1}{2}\frac{2\bar{b}}{a(\bar{\eta}_\nu) \cdot c(\bar{\eta}_\nu)\ T^*(\bar{\eta}_\nu)}\right)\bar{\gamma}_B(\bar{\eta}_\nu) = \frac{\alpha_B(T^*(\bar{\eta}_\nu) - 1)}{2T^*(\bar{\eta}_\nu)} + \sum_{n=1}^{m}{}' b_{\nu n}\bar{\gamma}_B(\bar{\eta}_n) \cdot \quad .. \quad (17)$$

Values of the fixed positions $\bar{\eta}_\nu$ and the coefficients $b_{\nu\nu}$ and $b_{\nu n}$ are given in Refs. 9 and 11.

The values of α_W, a, c are known along the span of the given wing. They have to be determined at the fixed points $\bar{\eta}_\nu$. The relation between $\bar{\eta}_\nu$ and the spanwise co-ordinate $\eta_\nu = y_\nu/\frac{1}{2}b$ on the given wing is given by the conformal transformation. For circular and elliptical body cross-sections the transformation is given in Ref. 4.

If the cross-section of the body is a circle of radius R:

$$\bar{u} = u + \frac{R^2}{u} \quad .. \quad .. \quad .. \quad .. \quad .. \quad (18)$$

so that for a symmetrically placed wing

$$\bar{y} = y - \frac{R^2}{y}$$

and

$$\eta = \frac{1}{2}\frac{\bar{b}}{b}\bar{\eta} + \sqrt{\left[\left(\frac{R}{b/2}\right)^2 + \left(\frac{1}{2}\frac{\bar{b}}{b}\bar{\eta}\right)^2\right]} \cdot \quad .. \quad .. \quad .. \quad (19)$$

The span in the $\bar{u}$-plane is

$$\bar{b} = b\left[1 - \left(\frac{R}{b/2}\right)^2\right] \quad .. \quad .. \quad .. \quad .. \quad .. \quad (20)$$

$$T(y) = 1 + \frac{R^2}{y^2}$$

and

$$T^*(y) = 1 + k\frac{R^2}{y^2} \quad .. \quad .. \quad .. \quad .. \quad .. \quad (21)$$

with

$$k = 1 - \frac{2}{\pi}\sin^{-1}\frac{t}{2R} - \frac{2}{\pi}\frac{t}{2R}\sqrt{\left[1 - \left(\frac{t}{2R}\right)^2\right]} \quad .. \quad .. \quad .. \quad (22)$$

where t is the wing-root thickness. In most cases this can be replaced by

$$k = 1 - \frac{2}{\pi}\frac{t}{R} \cdot \quad .. \quad .. \quad .. \quad .. \quad .. \quad .. \quad .. \quad (23)$$

If the cross-section of the body is an ellipse with height and width $2A'$ and $2B'$, respectively, the transformation is given by:—

$$\bar{u} = \frac{1}{A' - B'}[A'u - B' \sqrt{(u^2 - A'^2 + B'^2)}] . \quad .. \quad .. \quad (24)$$

This results from an intermediary transformation of the flow around the ellipse (u-plane) into the flow around a circle of radius R_1 (u_1-plane):

$$u = u_1 + \frac{A'^2 - B'^2}{4u_1}$$

$$R_1 = \frac{A' + B'}{2}$$

followed by the transformation of the u_1-plane into the $\bar{u}$-plane

$$\bar{u} = u_1 + \frac{R_1^2}{u_1} .$$

For a symmetrically placed wing

$$\bar{y} = \frac{y}{A' - B'}\left[A' - B' \frac{\sqrt{(y^2 + A'^2 - B'^2)}}{y}\right] \quad .. \quad .. \quad (25)$$

and

$$T(y) = \frac{1}{A' - B'}\left[A' - B' \frac{\sqrt{(y^2 + A'^2 - B'^2)}}{y + \frac{A'^2 - B'^2}{y}}\right]$$

$$T^*(y) = 1 + k\frac{B'}{A' - B'}\left[1 - \frac{\sqrt{(y^2 + A'^2 - B'^2)}}{y + \frac{A'^2 - B'^2}{y}}\right] . \quad .. \quad .. \quad (26)$$

From the values of $\bar{\eta}_\nu$ the y_ν can thus be determined and hence $\alpha_W(\bar{\eta}_\nu)$, $c(\bar{\eta}_\nu)$ and $T^*(\bar{\eta}_\nu)$. The local sectional lift slope $a(\eta)$ and thus $a(\bar{\eta}_\nu)$ can be worked out as shown in Ref. 11 for an isolated swept wing.

As all the coefficients in the systems of equations (16) and (17) are known, the unknown values of $\bar{\gamma}_W$ and $\bar{\gamma}_B$ can be worked out. This may be done by successive approximations*, as explained in Refs. 9 and 11. From $\bar{\gamma}_W$ and $\bar{\gamma}_B$ the loading over the original wing outside the body can be obtained from

$$\gamma(\eta) = \bar{\gamma}(\bar{\eta})\frac{\bar{b}}{b} . \quad .. \quad .. \quad .. \quad .. \quad .. \quad (27)$$

5. *The Load Distribution over the Body.*—5.1. *Lift Induced by the Wing.*—We consider first only the lift induced by the wing on the part of the body near the wing, *i.e.*, we do not consider any effects at the nose and the tail of the body.

* It will be sufficient in most cases to use 15 pivotal points along the span ($m = 15$) for $\bar{\gamma}_W$. For $\bar{\gamma}_B$, which usually changes rapidly near the wing-body junction, the use of more points ($m = 31$) is recommended in that region.

Whereas the load on the wing has been obtained from the lift force on the bound vortices by considering the distribution of trailing vorticity in the wake, a similar procedure cannot be followed to determine the load on the body. As illustrated in Fig. 6 the bound vortices of the wing will run across the surface of the body, joined by another system of bound vorticity on the body of, in general, opposite sense. Trailing vortices, whose strength varies around the circumference, are shed from the body and are found on the circle far behind the wing. Their strength is zero at the highest and lowest points of the circle and they are of opposite sign at corresponding points on the right- and left-hand sides of the circle. Thus in transforming the circle into a vertical slit, two corresponding vortices fall on top of each other and cancel out. This is, of course, the reason why the calculation of the flow is so much more easily done in the transformed plane. It implies, however, that the trailing vorticity on the body cannot be determined in the transformed plane.

Another way of determining the load on the body is to relate the integrated difference in pressure on the upper and lower surfaces of the body to the potential difference at certain points in the wake. Consider a section of the fuselage in a plane parallel to the plane of symmetry, as in Fig. 7. The local lift is equal to the difference between the pressure coefficients C_p on upper and lower surface, and the total lift coefficient C_L at that spanwise station, y, can be found by integrating the pressure difference along x from far upstream to far downstream of the wing.

$$C_L = \int_{-\infty}^{+\infty} -(C_{p\,\mathrm{US}} - C_{p\,\mathrm{LS}})\, d\left(\frac{x}{c}\right)$$

The suffixes US and LS denote upper and lower surface. The pressure coefficient is to a first order equal to twice the velocity increment v_x, which in turn is equal to the partial derivative of the potential function ϕ of the additional flow produced by wing and body:—

$$C_p = -2\frac{v_x}{V_0} = -\frac{2}{V_0}\frac{\partial\phi}{\partial x}.$$

Thus

$$C_L = \frac{2}{cV_0}\left[\phi_{\mathrm{US}}(x=\infty) - \phi_{\mathrm{LS}}(x=\infty)\right].$$

The difference $\phi_{\mathrm{US}} - \phi_{\mathrm{LS}}$ can be calculated in the $\bar{u}$-plane, since it does not alter with a conformal transformation.

So far the potential has been determined only on the wing, where

$$\phi(\bar{z}_W)_{\mathrm{US}} - \phi(\bar{z}_W)_{\mathrm{LS}} = \Gamma$$

and

$$\left(\frac{\partial\phi}{\partial\bar{z}}\right)_{\bar{z}=\bar{z}_W} = \bar{v}_{zi}(\bar{z}_W, x=\infty)$$

and the calculation method (equation (9)) is only suited to determine the values there. To find the potential at points on the vertical slit would be complicated and tedious. However, as there are no singularities outside the wing, $\phi(\bar{z})$ can be expanded in a power series with respect to $\bar{z} - \bar{z}_W$, where $\bar{z}_W$ corresponds to the junction with the thin wing; if only the first-order term is taken*,

$$\phi(\bar{z}) = \phi(\bar{z}_W) + \left(\frac{\partial\phi}{\partial\bar{z}}\right)_{\bar{z}=\bar{z}_W} \times (\bar{z} - \bar{z}_W).$$

* In the case of minimum induced drag where the downwash is constant along span, the potential at the slit can be determined more easily. It is found that the quadratic term in the above series modifies the lift reduction in the plane of symmetry, where the error is greatest, by a factor $1 - 2D/b$.

Thus only the potential at the wing junction need be known. With the relations above,

$$C_L = \frac{2\Gamma(\bar{\eta}=0)}{cV_0} + 2\frac{\bar{v}_{zi}(\bar{z}_W, x=\infty)}{V_0}\frac{(\bar{z}_{US}-\bar{z}_W)-(\bar{z}_{LS}-\bar{z}_W)}{c}.$$

The values of $\bar{z}_{US}$ and $\bar{z}_{LS}$ for a certain section of the fuselage can be found from the transformation $\bar{u}(u)$. For a circular body cross-section and a symmetrically placed wing ($z_W = \bar{z}_W = 0$) we obtain

$$\bar{z} = 2z = 2R\sqrt{\left[1-\left(\frac{y}{R}\right)^2\right]}$$

so that finally for the load distribution over the body attached to a thin wing:

$$\gamma(y) = \frac{C_L \cdot c}{2b} = \bar{\gamma}(\bar{\eta}=0)\frac{\bar{b}}{b} - 2\frac{\bar{v}_{zi}(\bar{\eta}=0, x=\infty)}{V_0}\frac{R}{b/2}\sqrt{\left[1-\left(\frac{y}{R}\right)^2\right]}. \quad .. \quad (28)$$

In this relation the downwash is determined by the known load distribution:

$$\frac{\bar{v}_{zi}(\bar{\eta}=0, x=\infty)}{V_0} = \bar{a}_i(\bar{\eta}=0, x=\infty) = \frac{1}{2\pi}\int_{-1}^{+1}\frac{d\bar{\gamma}}{d\bar{\eta}'}\frac{d\bar{\eta}'}{\bar{\eta}-\bar{\eta}'}$$

$$= 2[b_{\nu\nu}\bar{\gamma}_\nu - \Sigma' b_{\nu n}\bar{\gamma}_n]. \quad .. \quad .. \quad .. \quad .. \quad .. \quad (29)$$

Thus the linear variation of the potential along the slit causes an elliptical distribution of the lift reduction across the body.

The reduction of the load over the body width from the junction to the centre-line is less for the thick wing than the value given by equation (28) for the thin wing. We take account of this fact by replacing R by $\sqrt{k}R$, as we have done in equations (8) and (10). If the body diameter is equal to the wing thickness, $k = 0$, the load is assumed constant across the body. For bodies with elliptical cross-section, the radius R in equation (28) has to be replaced by $\frac{1}{2}(A' + B')$.

5.2. *Change of Download at the Tail.*—We now consider the normal forces near the nose and the tail of the body. To a first approximation the wing does not affect the flow near the nose and so the lift there is unaltered. But the trailing vortices alter the effective angle of incidence of the flow at the rear end of the body and so affect the download. This gives a change of total lift which has to be added to the lift induced by the wing on the part of the body near the wing.

An estimate for the download acting on the tail of the isolated body can be obtained by integrating equation (1):

$$\frac{L}{\frac{1}{2}\rho V_0^2} = -2\alpha_{B\,\mathrm{eff}}A \quad .. \quad .. \quad .. \quad .. \quad .. \quad (30)$$

where A is the maximum cross-section area of the body and $\alpha_{B\,\mathrm{eff}}$ the effective incidence of the body. The coefficient for the download at the tail of a body of circular cross-section referred to the wing area is:

$$C_L = \frac{L}{\frac{1}{2}\rho V_0^2 b\bar{c}} = -\alpha_{B\,\mathrm{eff}} \cdot \frac{\pi}{2} \cdot \frac{(D/\bar{c})^2}{\mathrm{AR}} \quad .. \quad .. \quad .. \quad .. \quad (31)$$

where $\bar{c}$ is the mean wing chord and AR the aspect ratio of the wing.

To obtain a second estimate for the download at the tail of the body, we use the calculated moments of ellipsoids in parallel flow, *see, e.g.*, Vandrey[13] (1940). The moment is:

$$\frac{M}{\frac{1}{2}\rho V_0^2} = \frac{4}{3}\pi A'B'C' \,.\, 2\alpha_{B\,\mathrm{eff}} m\left(\frac{C'}{A'}, \frac{B'}{C'}\right) \quad .. \quad .. \quad .. \quad .. \quad (32)$$

where A', B' and C' are the semi-axes of the ellipsoid. Values of the function $m(C'/A', B'/C')$ are given in Fig. 8. Assuming a lift L at the nose and a download $-L$ at the tail, acting at points which are at a distance $l/2$ away from the centre of the body, they produce a moment

$$M = L \,.\, l \,.$$

Thus the download on a body of circular cross-section is given by:

$$C_L = -\alpha_{B\,\mathrm{eff}} \frac{\pi}{3} \frac{l_B}{l} \frac{(D/\bar{c})^2}{\mathrm{AR}} m\left(\frac{C'}{A'}, 1\right)$$

where l_B is the body length. For the body of circular section and high fineness ratio m will be about $0{\cdot}9$ (Fig. 8) and an approximate value of l/l_B will be $0{\cdot}75$, so that:

$$C_L = -\alpha_{B\,\mathrm{eff}} \,.\, 0{\cdot}8 \frac{\pi}{2} \,.\, \frac{(D/\bar{c})^2}{\mathrm{AR}}, \quad .. \quad .. \quad .. \quad .. \quad (33)$$

i.e., $0{\cdot}8$ times the value estimated by equation (31). The greater value of the first estimate, equation (31), can partly be explained by the fact that equation (1) overestimates the load near the stagnation point (*see* Fig. 1).

If the trailing vortices produce at the rear part of the body a downwash α_i, then the effective incidence and the amount of download at the body are reduced and the lift of the wing-body combination is increased. Using the estimate of equation (31), we have

$$\Delta C_L = \alpha_i \frac{\pi}{2} \frac{(D/\bar{c})^2}{\mathrm{AR}} \,. \quad .. \quad .. \quad .. \quad .. \quad .. \quad (34)$$

α_i varies across the body. At the wing-body junction of a thin wing attached to a circular body, α_i is equal to twice the value $\bar{a}_i$ given by equation (29) ; in the plane of symmetry, $\alpha_i = 0$. To obtain a mean value it is suggested that α_i is taken as equal to $\bar{a}_i$ from equation (29).

The lift on the body as determined by equation (28) together with the increment ΔC_L from equation (34) is what might be expected in non-viscous flow. A further lift increment arises in viscous flow. The vertical component of the skin-friction forces on the body produce a lift increment, as has been pointed out by Multhopp[4]. The additional lift depends on the square of the incidence and is therefore small at low values of C_L .

A further effect of the viscous flow round the body is to give a thicker boundary layer above than below ; this effect intensifies as the point considered is further back on the body and has the effect of reducing the effective incidence still further. In consequence, the lift near the nose is little affected but the download at the tail may be much reduced. Particularly at low Reynolds numbers, there may even be a breakaway of the flow at the rear of the body, in which case all the download may be lost, so that the overall increase in lift is given by:

$$\Delta C_L = \alpha_B \,.\, \frac{\pi}{2} \frac{(D/\bar{c})^2}{\mathrm{AR}} \quad .. \quad .. \quad .. \quad .. \quad .. \quad (35)$$

from equation (31).

6. *Examples of Calculation Method.*—In Fig. 9* the results of the present method are compared with those of Multhopp's method for thin wings in a particular case. The effect of the fuselage is smaller according to the present calculation, due to the finite chord of the wing (full downwash for $\bar{\gamma}_B$ in equation (14)) and to a lesser degree, due to the thickness of the wing (from the factor k in equation (10) ; in this case $k = 0{\cdot}57$). Experimental values of the lift induced on the body by the wing, integrated from measured pressure coefficients, are also plotted in Fig. 9 and show good agreement with the calculated values.

Figs. 10 and 11 give the calculated values of overall lift change due to a body on a straight and a 45-deg sweptback wing of aspect ratio 3. Of the three curves given, (*a*) denotes the calculation which includes only the load induced on the body near the wing, (*b*) includes the effect of wing downwash on the tail load, from equation (34), and for (*c*) it has been assumed that, due to viscous effects, equation (35), there is no download on the tail of the body.

The calculated span loadings for a series of bodies and wings having 0 deg and 45 deg of sweepback are shown in Figs. 12 and 13 for symmetrical arrangements. Only the lift induced on the body near the wing is considered. It will be seen that the effect of sweepback is to modify the basic wing distribution and to reduce the decrease of lift over the fuselage because of the much smaller downwash in the junction (*see* Fig. 13). The overall lift change $\Delta \bar{C}_L$ due to the body has been calculated for the same series of bodies and is plotted in Fig. 15. This shows that for large bodies on small aspect ratio wings, the lift increase over the wing may be cancelled by the loss of induced lift over the body. The overall lift difference then depends only on the download at the tail of the body.

In view of the many parameters involved it is not possible to generalise these results, and any given wing-body arrangement has to be calculated anew. This does not, however, present any particular difficulties, since the calculation procedure is simple and can be performed in about one day.

The overall lift slope of the wing-body combination is in itself not very informative as to the actual loads ; in many cases the overall change in lift may be very small whereas there is an appreciable lift increment on the wing, compensated by a smaller load on the body. With swept-back wings in particular an overall increase of the lift due to the body is often observed. A reduction of the overall lift is usually caused by the body being set at a smaller angle of incidence than the wing. To illustrate this, Fig. 16 shows the effect of a wing-body angle i , on the load distribution ; the additional lift due to the different junction shapes is not taken into account. Comparing the results for $i = 4$ deg with those for $i = 0$ deg clearly shows the lift reduction which is particularly noticeable at small lift coefficients. In this example, the lift distribution over the wing is about the same as that of the wing alone for a wing incidence $\alpha_W = 6$ deg. This type of loading has often been considered as being a general characteristic of wing-body interference. We find, however, that this occurs only in very special cases.

7. *Results from Systematic Model Tests*[14].—Some experimental data are available for a systematic series of bodies attached to straight cambered wings of aspect ratios 5 and 10, taper ratio 2:1 ; for details *see* Anscombe and Raney[14] (1949). Only the effect on the total lift has been measured.

Bodies with the same centre part ($D/\bar{c} = 0{\cdot}9$) but with nose and tail extensions of varying length were tested. The lift increments for a midwing arrangement are shown in Fig. 17. The spacing of the lines enclosing the band of points corresponds to $\pm 0{\cdot}05$ deg incidence, this represents the accuracy of the tests. No effect of the body length can be seen ; this independence of body length was assumed in the calculation method.

* A lift slope of $a_0 = 0{\cdot}75 \, . \, 2\pi$ has been used in the calculations of Figs. 9, 10 and 11, since this value corresponds to the measured total lift coefficient $\bar{C}_L/\alpha = 3{\cdot}0$ of the wing alone.

Mean values of the change in lift slope from the tests with different front and rear lengths are given in Table 1 and plotted for the mid-wing in Fig. 18. Calculated values (*a*), (*b*), (*c*), as explained in section 6, are also plotted. The loading of the wing alone is nearly elliptical ; since this is usually the case for unswept wings of large or fairly large aspect ratio, the data are applicable to transport-type aircraft with thick wing roots.

The data are of further interest since they show how large the effect of the difference in junction shape on the upper and lower surface can be. Fig. 17 shows that a change in wing-body angle causes a lift reduction $\Delta\bar{C}_{L0}$ independent of incidence. Mean values of $\Delta\bar{C}_{L0}$ for the various body lengths are given in Table 1 and show that $\Delta\bar{C}_{L0}$ is 0·01 more negative for each degree of wing-body angle. The calculated value (case (*b*)) is $-0{\cdot}006$. The difference between the measured and the calculated values is due to the different junction shapes, which are not taken into account in the calculation. It is not possible to generalize these results, since they depend on the wing section ; the model had a cambered wing, which was 18 per cent thick at the root.

8. *Conclusions.*—Experiments have proved that beyond a certain body length the lift distribution over a wing-body combination is independent of the body length. Therefore, for calculating the spanwise lift distribution over the wing and the part of the body near the wing, an infinitely long body can be assumed. The effect of the wing on the tail of the body is considered separately. Multhopp's method[4] for calculating the lift distribution is extended to take account of:

(i) sweepback, by using the corresponding sectional lift slope varying along span, as explained in Ref. 11

(ii) the finite wing thickness, by reducing the upwash of the isolated body by a factor k

(iii) the finite ratio of root chord to body diameter, by taking the downwash on the wing as equal to the full downwash at infinity when calculating the effect of the twist due to the body upwash.

The wing induces a downwash at the tail of the body, reducing the download there and thus producing a lift increment approximately equal to $\alpha_i \frac{1}{2}\pi(D/\bar{c})^2/\mathrm{AR}$. For wings in an off-centre position or at an angle to the body axis an additional lift is produced by the difference in junction shapes ; this lift increment, which does not change with incidence cannot be calculated by this method.

REFERENCES

No.	*Author*	*Title, etc.*
1	H. Schlichting	Aerodynamics of the mutual influence of aircraft parts (interference). Völkenrode R. & T. No. 171. August, 1946. R.A.E. Library Translation No. 275. A.R.C. 12,669. October, 1948.
2	A. H. Flax and H. R. Lawrence ..	The aerodynamics of low-aspect-ratio wings and wing-body combinations. Proc. Third Anglo-American Aeronaut. Conf., Brighton, 1951, p. 363.
3	H. V. Becker, H. B. Squire and C. Callen	The effect of fuselage and nacelles on wing bending moment, shear and torsion. R. & M. 2060. November, 1943.
4	H. Multhopp	Aerodynamics of the fuselage. *Luftfahrtforschung* Vol. 18, p. 52. 1941. RTP Translation No. 1220. A.R.C. 5263.
5	R. T. Jones	Properties of low-aspect-ratio pointed wings at speeds below and above the speed of sound. N.A.C.A. Report No. 835. 1946.
6	W. Liess and F. Riegels	Bemerkungen zum Rumpfeinfluss. Jahrbuch 1942 der deutschen Luftfahrtforschung, p.I, 366.
7	J. Lennertz	Beitrag zur theoretischen Behandlung des gegenseitigen Einflusses von Tragfläche und Rumpf. Z.A.M.M. Vol. 7, p. 249. 1927. Durand, Vol. IV, p. 152.
8	J. R. Spreiter	Aerodynamic properties of slender wing-body combinations at subsonic, transsonic, and supersonic speeds. N.A.C.A. Tech. Note 1662. July, 1948.
9	H. Multhopp	The calculation of the lift distribution of aerofoils. *Luftfahrtforschung* Vol. 15, p. 153. 1938. RTP Translation No. 2392. A.R.C. 8516.
10	J. Ginzel	Die Auftriebsverteilung eines tiefen verwundenen Rechteckflügels. Jahrbuch 1940 der deutschen Luftfahrtforschung, p.I, 238.
11	D. Küchemann	A simple method for calculating the span and chordwise loadings on thin swept wings. R.A.E. Report Aero. 2392. A.R.C. 13,758. 1950.
12	R.A.E. Wind Tunnel Staff	Low speed pressure distribution on a 59-deg swept wing and comparison with high speed results on a 45-deg swept wing. C.P. 86. February, 1949.
13	F. Vandrey	Abschätzung des Rumpfeinflusses auf das Längsmoment eines Flugzeuges. Jahrbuch 1940 der deutschen Luftfahrtforschung p.I, 367.
14	A. Anscombe and D. J. Raney ..	Low-speed tunnel investigation of the effect of the body on C_{m0} and aerodynamic centre of unswept wing-body combinations. C.P. 16. April, 1949.

LIST OF SYMBOLS

x,y,z		Rectangular system of co-ordinates, x in wind direction, y sideways, z downwards
$\bar{y},\bar{z}$		Co-ordinates in the transformed Trefftz-plane
u	$=$	$z + iy$. Complex variable in the Trefftz-plane
$\bar{u}$	$=$	$\bar{z} + i\bar{y}$. Complex variable in the transformed Trefftz-plane
η	$=$	$\frac{y}{b/2}$
$\bar{\eta}$	$=$	$\frac{\bar{y}}{\bar{b}/2}$
c		Local wing chord
$\bar{c}$		Mean wing chord
b		Wing span
$\bar{b}$		Wing span in the transformed Trefftz-plane
t		Wing thickness
R		Radius of fuselage with circular cross-section
D	$=$	$2R$
A', B', C'		Semi-axes of ellipse or ellipsoid, respectively
AR	$=$	$\frac{b}{\bar{c}}$. Aspect ratio
φ		Angle of sweep
α_W		Angle of incidence of the wing to the main flow
α_B		Angle of incidence of the body to the main flow
α_i		Induced angle of incidence
i		Wing-body angle, angle between body axis and zero-lift line of the wing
C_L		Local lift coefficient
$\bar{C}_L$		Overall lift coefficient
$\Delta\bar{C}_L$		Difference of the lift coefficients with and without body at the same incidence
$\Delta\bar{C}_{L0}$		Value of $\Delta\bar{C}_L$ for zero-lift angle of the wing alone
γ	$=$	$\frac{\Gamma}{b\bar{V}_0} = \frac{C_L c}{2b}$. Non-dimensional circulation
$\bar{\gamma}$	$=$	$\frac{\Gamma}{\bar{b}\bar{V}_0}$
γ_W		The part of γ that depends only on α_W
γ_B		The part of γ that depends only on α_B
a	$=$	$\frac{dC_L}{d\alpha}$ local lift slope without trailing vortices

a_0		Lift slope coefficient of the two-dimensional aerofoil
T	=	$R\left(\frac{d\bar{u}}{du}\right)$ real part of $\frac{d\bar{u}}{du}$
T^*	=	$1 + k(T - 1)$
k		Ratio of the body cross-section area above and below the wing to the total frontal area of the body
$b_{\nu\nu}$, $b_{\nu n}$		Coefficients
ν, n		Number of pivotal point

TABLE 1

Change in Lift due to Body

(*Extract from Ref.* 14)

Body tested	$\frac{D}{\bar{c}}$	$\frac{D}{b}$	Wing position	Height relative to body centre-line $z_{W/\frac{1}{2}D}$	Wing-body angle from No Lift (deg)	$\frac{\partial \Delta \bar{C}_L}{\partial \bar{C}_L}$	ΔC_{L0}
AR = 10							
9-in. diam.	0·909	0·091	High	0·556	2·1	0·045	−0·020
			Mid	0	2·1	0·044	−0·017
			Low (small fillets)	−0·688	2·1	0·043	−0·019
(The low wing agrees with high and mid if a minimum fillet is fitted. With no fillet or large fillets the changes in $\Delta \bar{C}_{L0}$ cannot be generalised.)							
			Mid	0	6·1	0·044	−0·058
9-in. × 13½-in.	0·909*	0·091*	Mid	0	2·1	0·044	−0·029
4½-in. diam.	0·454	0·045	Mid	0	2·1	0·020	−0·023
13½-in. diam.	1·363	0·136	Mid	0	2·35	0·074	−0·040
AR = 5							
4½-in. diam.	0·454	0·091	Mid	0	2·2	0·040	−0·013
9-in. diam.	0·909	0·182	Mid	0	2·2	0·058	−0·034

* In this case, the width of the body is used for D.

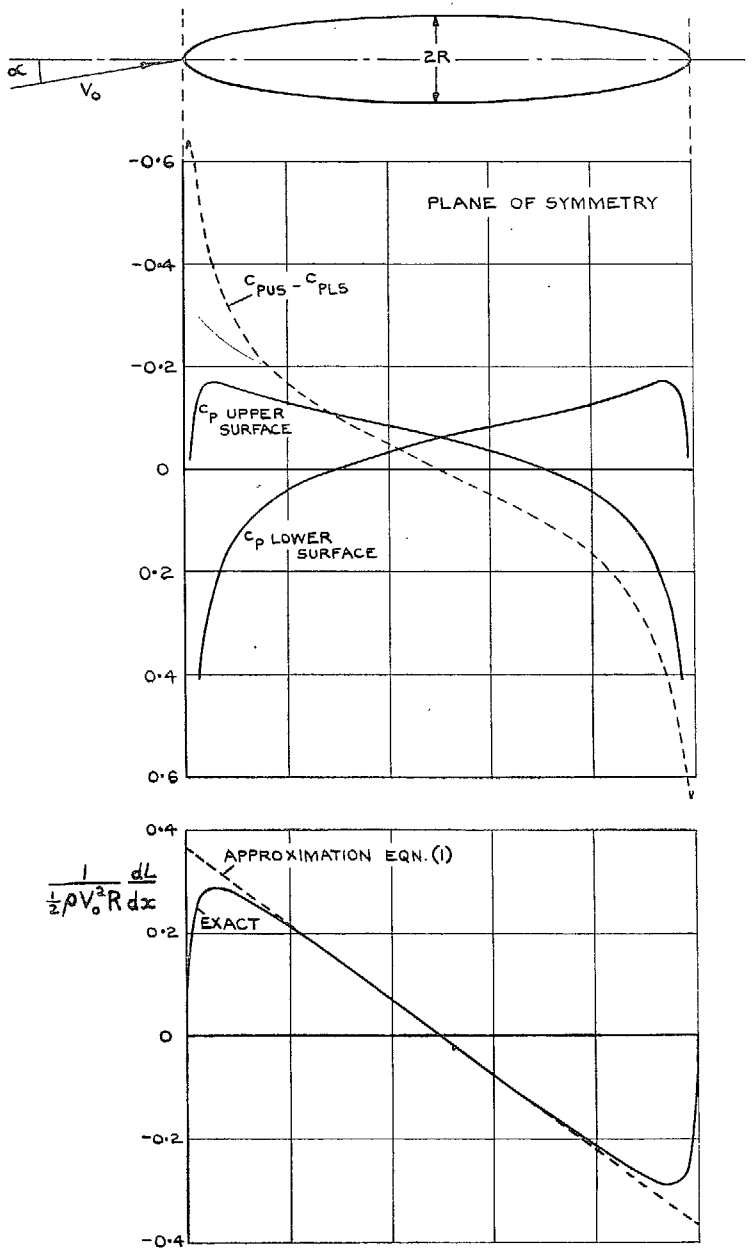

FIG. 1. Pressure and load distribution on axially symmetrical ellipsoid of fineness ratio 6. $\alpha = 10$ deg.

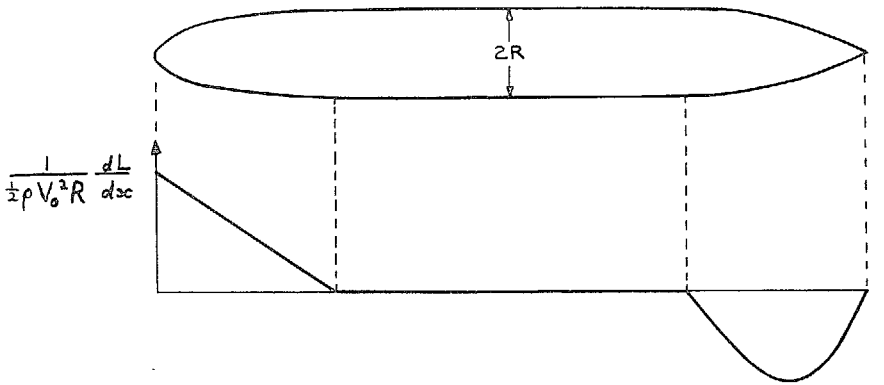

FIG. 2. Load distribution on isolated body with cylindrical middle part ; equation (1).

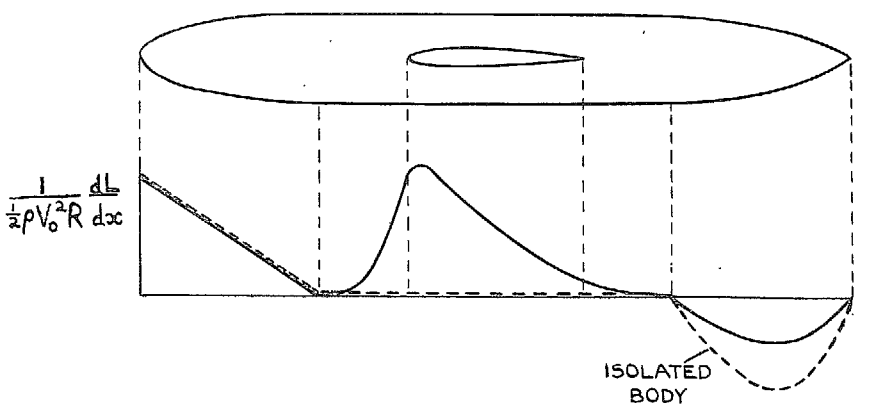

FIG. 3. Sketch of load distribution over body when attached to a wing.

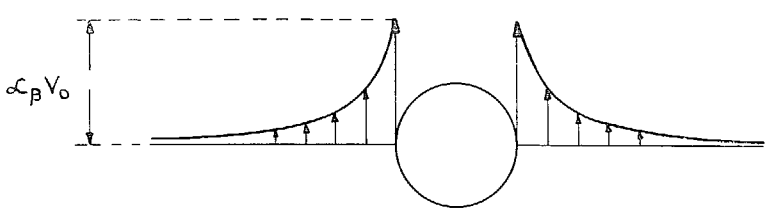

FIG. 4. Upwash produced by circular body.

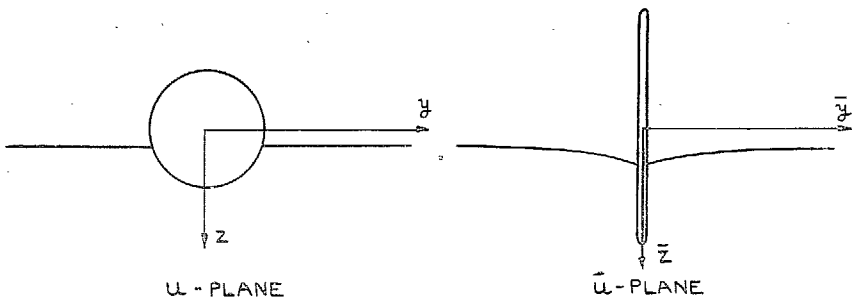

FIG. 5. Original and transformed Trefftz-plane.

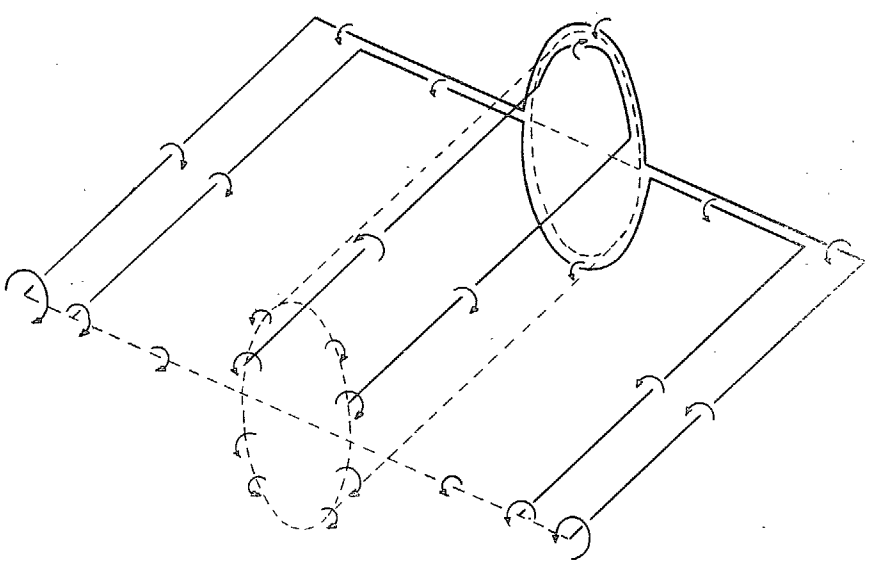

FIG. 6. Vortex system for wing-body combination.

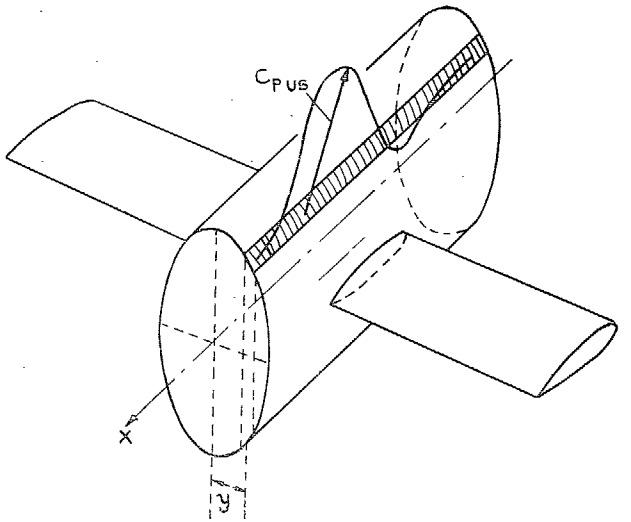

FIG. 7. Integration of pressure along body.

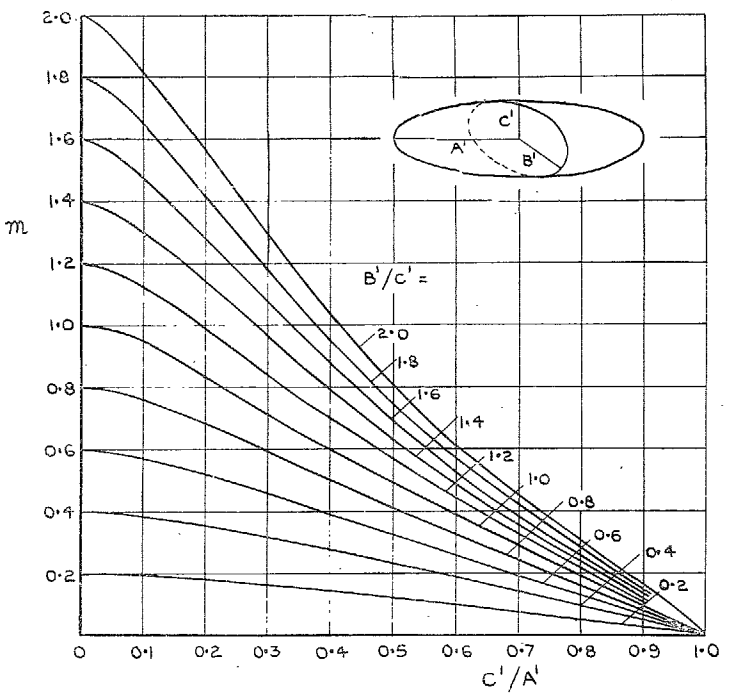

FIG. 8. A function used in the calculation of the unstable moment of ellipsoids. From Ref. 13.

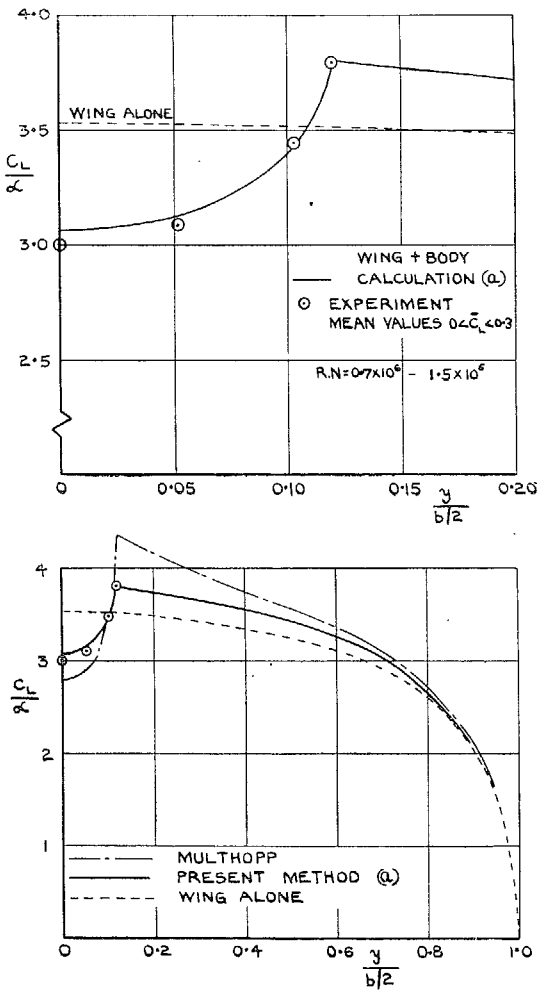

FIG. 9. Spanwise lift distributions. Cylindrical body on straight wing. AR = 3, $\varphi = 0$, taper ratio = 1·0, $D/c = 0{\cdot}36$, $t/c = 0{\cdot}12$, $a_0 = 0{\cdot}75 \times 2\pi$.

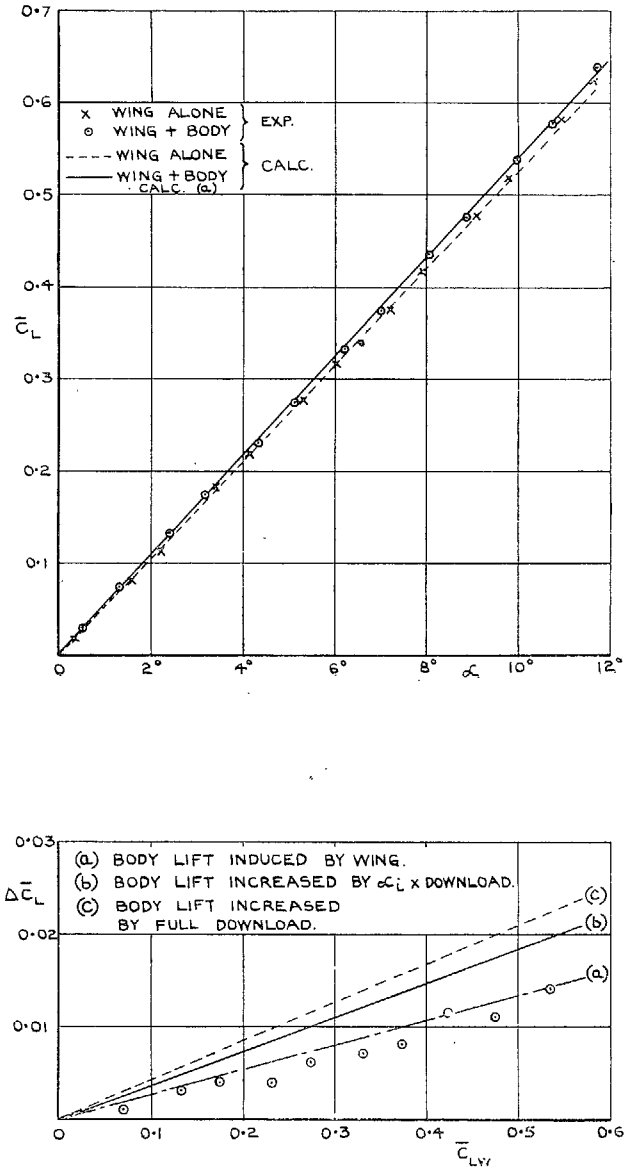

FIG. 10. Overall lift of cylindrical body ($D/c = 0{\cdot}36$) on straight wing. AR = 3, $\varphi = 0$, taper ratio = 1, $t/c = 0{\cdot}12$, Reynolds number = $0{\cdot}7 \times 10^6$.

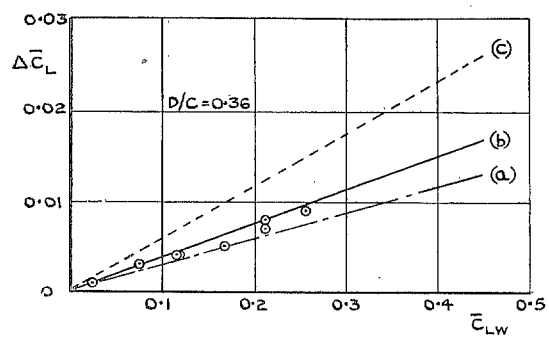

(a) BODY LIFT INDUCED BY WING

(b) BODY LIFT INCREASED BY α_L × DOWNLOAD

(c) BODY LIFT INCREASED BY FULL DOWNLOAD

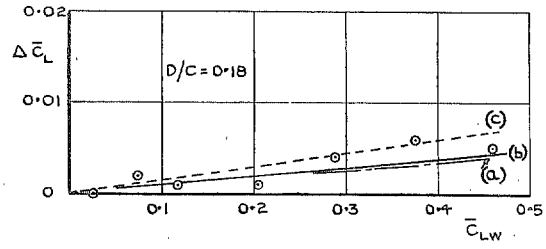

FIG. 11. Overall lift increment cylindrical bodies on swept wing.
AR = 3, $\varphi = 45$ deg, taper ratio = 1·0, $t/c = 0{\cdot}12$,
Reynolds number = $0{\cdot}7 \times 10^6$.

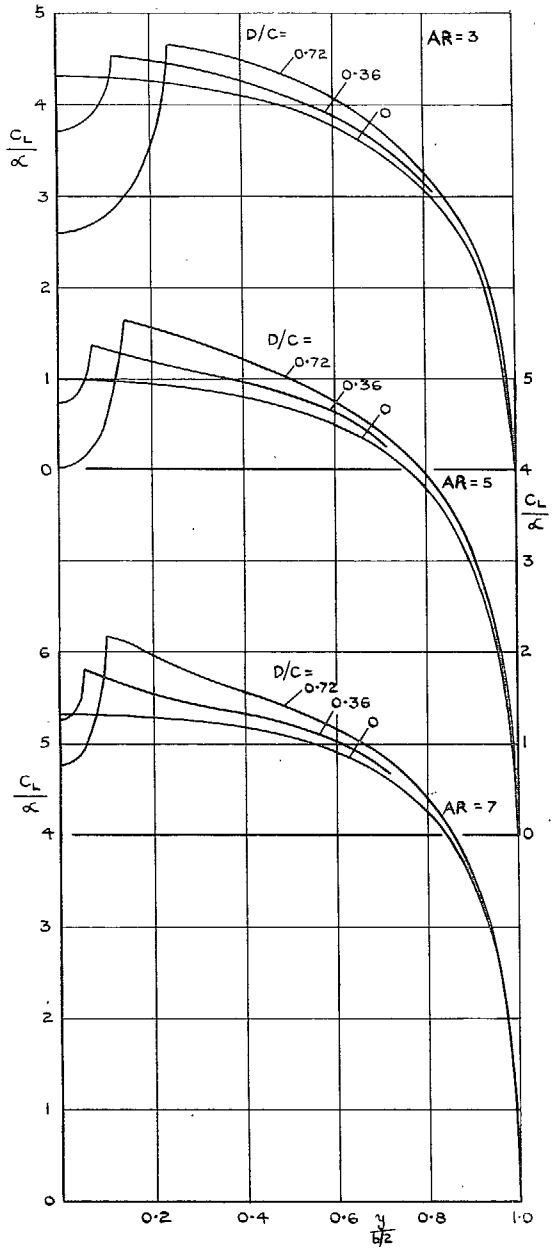

FIG. 12. Calculated spanwise lift distributions.
Straight wings, taper ratio $= 1{\cdot}0$, $t/c = 0{\cdot}12$, $a_0 = 2\pi$.

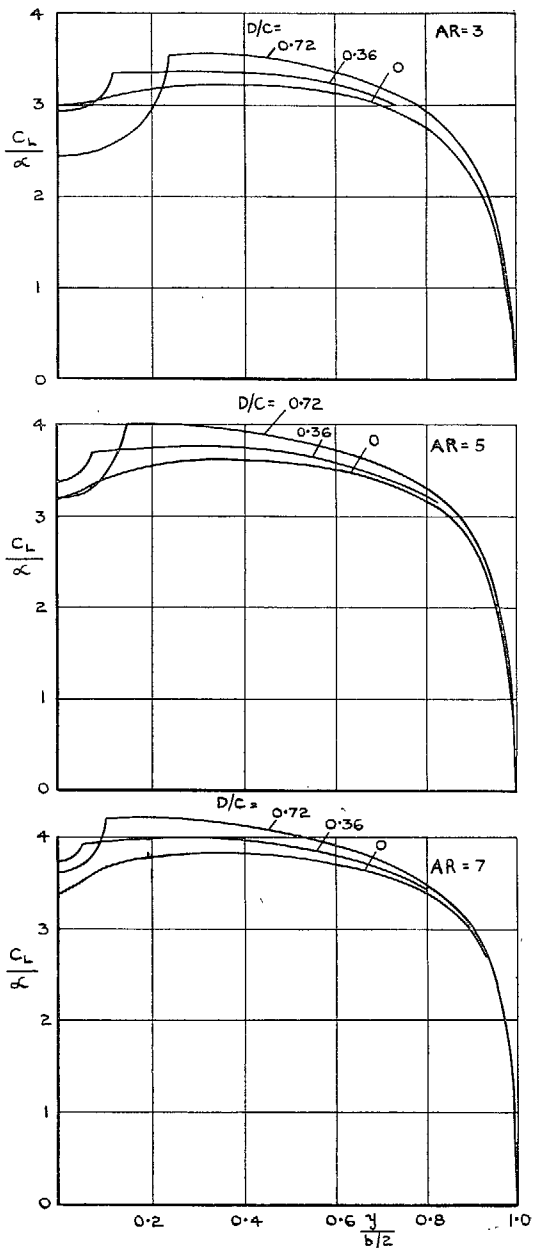

FIG. 13. Calculated spanwise lift distributions.
Swept wing, $\varphi = 45$ deg, taper ratio $= 1{\cdot}0$, $t/c = 0{\cdot}12$, $a_0 = 2\pi$.

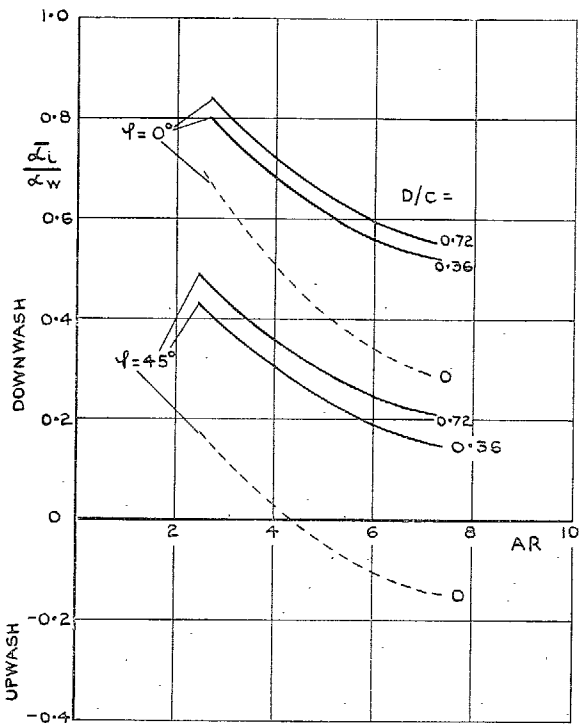

FIG. 14. Calculated downwash at the body junction in Trefftz-plane.

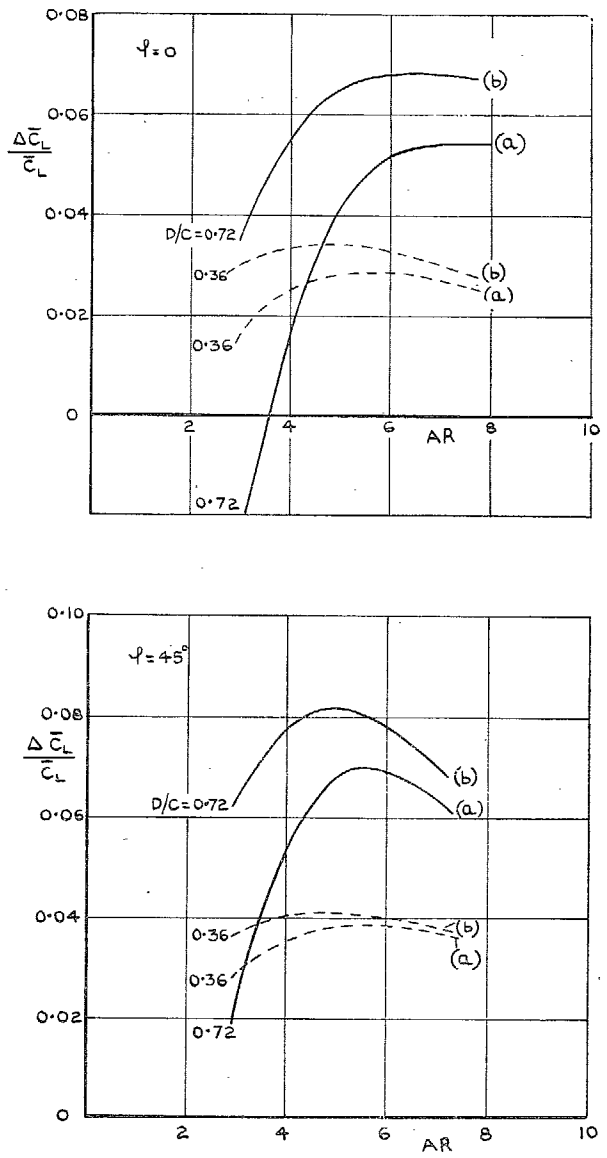

(a) BODY LIFT INDUCED BY WING.

(b) BODY LIFT INCREASED BY α_L × DOWNLOAD.

FIG. 15. Overall lift increment, from Figs. 12 and 13.

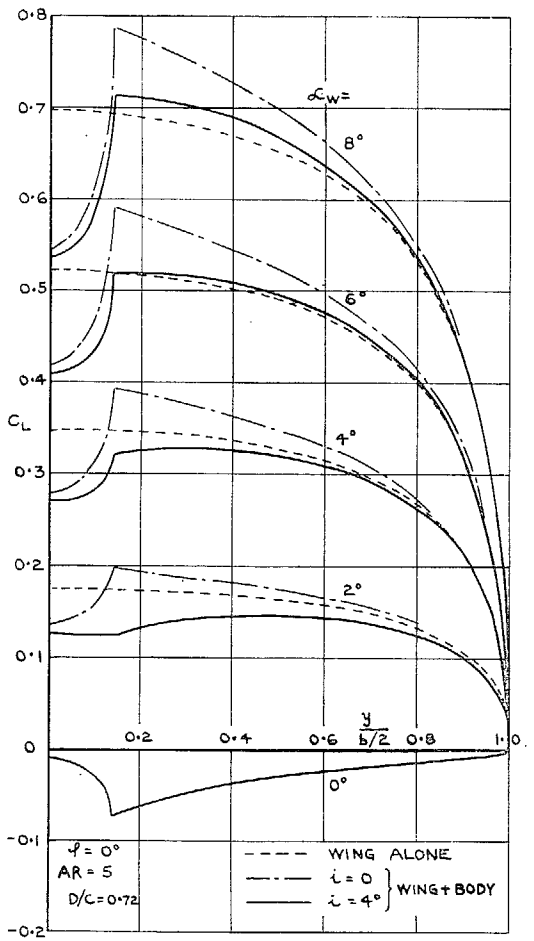

FIG. 16. Effect of a wing-body angle on the load distribution.

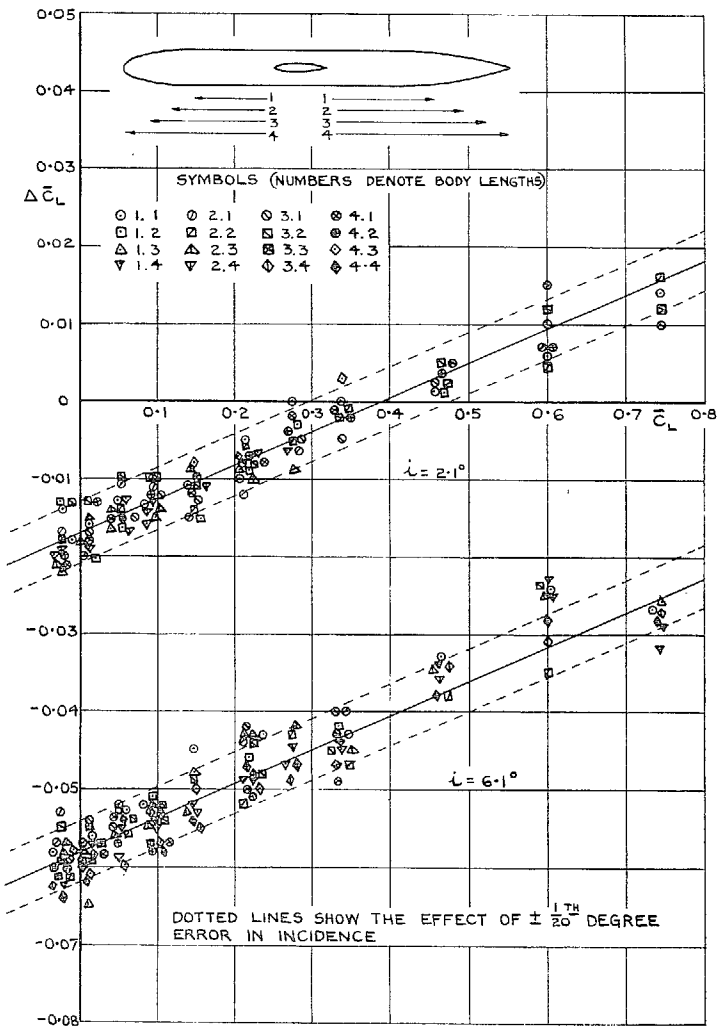

D/c̄ = 0·91 , AR = 10 , TAPER RATIO 2:1
t/c = 0·18 AT CENTRE, 0·12 AT TIP.
MID WING

FIG. 17. Overall lift increment due to body.

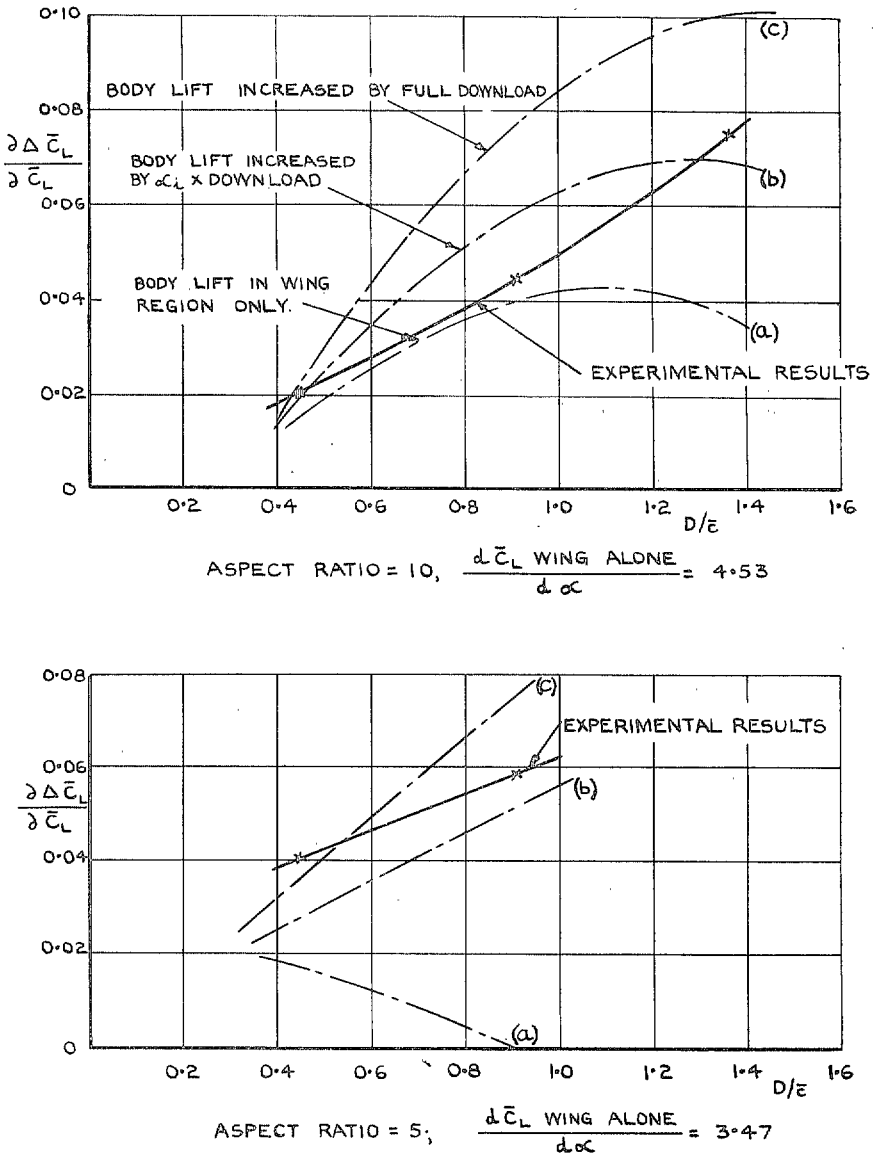

FIG. 18. Overall lift increment with unswept wings of aspect ratio 5 and 10.

Printed in Great Britain under the authority of Her Majesty's Stationery Office
By The Hove Printing Co., Ltd.

(6706) Wt. 18/680 K.7 12/56 H.P.Co. 34-261

Publications of the Aeronautical Research Council

ANNUAL TECHNICAL REPORTS OF THE AERONAUTICAL RESEARCH COUNCIL (BOUND VOLUMES)—

1939 Vol. I. Aerodynamics General, Performance, Airscrews, Engines. 50*s.* (51*s.* 9*d.*)
Vol. II. Stability and Control, Flutter and Vibration, Instruments, Structures, Seaplanes, etc. 63*s.* (64*s.* 9*d.*)

1940 Aero and Hydrodynamics, Aerofoils, Airscrews, Engines, Flutter, Icing, Stability and Control, Structures, and a miscellaneous section. 50*s.* (51*s.* 9*d.*)

1941 Aero and Hydrodynamics, Aerofoils, Airscrews, Engines, Flutter, Stability and Control, Structures. 63*s.* (64*s.* 9*d.*)

1942 Vol. I. Aero and Hydrodynamics, Aerofoils, Airscrews, Engines. 75*s.* (76*s.* 9*d.*)
Vol. II. Noise, Parachutes, Stability and Control, Structures, Vibration, Wind Tunnels. 47*s.* 6*d.* (49*s.* 3*d.*)

1943 Vol. I. Aerodynamics, Aerofoils, Airscrews. 80*s.* (81*s.* 9*d.*)
Vol. II. Engines, Flutter, Materials, Parachutes, Performance, Stability and Control, Structures. 90*s.* (92*s.* 6*d.*)

1944 Vol. I. Aero and Hydrodynamics, Aerofoils, Aircraft, Airscrews, Controls. 84*s.* (86*s.* 3*d.*)
Vol. II. Flutter and Vibration, Materials, Miscellaneous, Navigation, Parachutes, Performance, Plates and Panels, Stability, Structures, Test Equipment, Wind Tunnels. 84*s.* (86*s.* 3*d.*)

1945 Vol. I. Aero and Hydrodynamics, Aerofoils. 130*s.* (132*s.* 6*d.*)
Vol. II. Aircraft, Airscrews, Controls. 130*s.* (132*s.* 6*d.*)
Vol. III. Flutter and Vibration, Instruments, Miscellaneous, Parachutes, Plates and Panels, Propulsion. 130*s.* (132*s.* 3*d.*)
Vol. IV. Stability, Structures, Wind Tunnels, Wind Tunnel Technique. 130*s.* (132*s.* 3*d.*)

ANNUAL REPORTS OF THE AERONAUTICAL RESEARCH COUNCIL—

1937 2*s.* (2*s.* 2*d.*) 1938 1*s.* 6*d.* (1*s.* 8*d.*) 1939–48 3*s.* (3*s.* 3*d.*)

INDEX TO ALL REPORTS AND MEMORANDA PUBLISHED IN THE ANNUAL TECHNICAL REPORTS, AND SEPARATELY—

April, 1950 . . . . . R. & M. No. 2600 2*s.* 6*d.* (2*s.* 8*d.*)

AUTHOR INDEX TO ALL REPORTS AND MEMORANDA OF THE AERONAUTICAL RESEARCH COUNCIL—

1909–January, 1954 . . . R. & M. No. 2570 15*s.* (15*s.* 6*d.*)

INDEXES TO THE TECHNICAL REPORTS OF THE AERONAUTICAL RESEARCH COUNCIL—

December 1, 1936 — June 30, 1939	R. & M. No. 1850	1*s.* 3*d.* (1*s.* 5*d.*)
July 1, 1939 — June 30, 1945	R. & M. No. 1950	1*s.* (1*s.* 2*d.*)
July 1, 1945 — June 30, 1946	R. & M. No. 2050	1*s.* (1*s.* 2*d.*)
July 1, 1946 — December 31, 1946	R. & M. No. 2150	1*s.* 3*d.* (1*s.* 5*d.*)
January 1, 1947 — June 30, 1947	R. & M. No. 2250	1*s.* 3*d.* (1*s.* 5*d.*)

PUBLISHED REPORTS AND MEMORANDA OF THE AERONAUTICAL RESEARCH COUNCIL—

Between Nos. 2251–2349	R. & M. No. 2350	1*s.* 9*d.* (1*s.* 11*d.*)
Between Nos. 2351–2449	R. & M. No. 2450	2*s.* (2*s.* 2*d.*)
Between Nos. 2451–2549	R. & M. No. 2550	2*s.* 6*d.* (2*s.* 8*d.*)
Between Nos. 2551–2649	R. & M. No. 2650	2*s.* 6*d.* (2*s.* 8*d.*)

Prices in brackets include postage

HER MAJESTY'S STATIONERY OFFICE

York House, Kingsway, London, W.C.2; 423 Oxford Street, London, W.1 (Post Orders: P.O. Box 569, London, S.E.1); 13a Castle Street, Edinburgh 2; 39 King Street, Manchester 2; 2 Edmund Street, Birmingham 3; 109 St. Mary Street, Cardiff; Tower Lane, Bristol 1; 80 Chichester Street, Belfast *or through any bookseller.*

S.O. Code No. 23-2872